ACS Macro Letters

Letter

pubs.acs.org/macroletters

Ultraviolet Light-Induced Surface-Initiated Atom-Transfer Radical Polymerization

Junfeng Yan, Bin Li, Feng Zhou,* and Weimin Liu

State Key Laboratory of Solid Lubrication, Lanzhou Institute of Chemical Physics, Chinese Academy of Sciences, Lanzhou 730000, China

Supporting Information

ABSTRACT: UV light-induced surface-initiated atom-transfer radical polymerization (ATRP) was reported. This method uses TiO_2 nanoparticles as photoactive materials to reduce Cu(II)/L to a Cu(I)/L complex under UV irradiation by a one-electron transfer process for ATRP with multiple usage of monomer solutions. The growth of polymer brushes can be manipulated by either varying the content of photoactive materials or regulating the irradiation intensity, thereby yielding polymer brushes with controllable thickness, composition, and architecture.

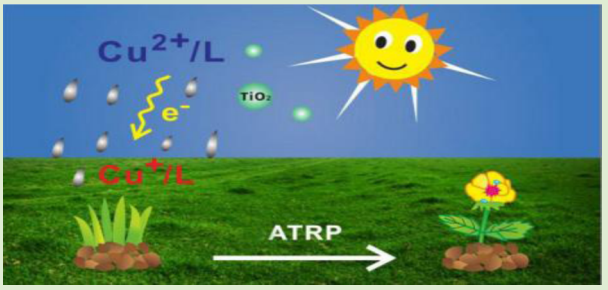

Polymer brushes produced by controlled or living surface-initiated radical polymerization[1,2] provide a superior route for surface functionalization, such as creation of smart surfaces,[3−5] antibiofouling materials,[6,7] and lubrication.[8] Compared with various controlled radical polymerization techniques[9] and organic polymer synthesis strategies,[10] atom-transfer radical polymerization (ATRP)[11−14] facilitates the construction of diverse polymer assemblies.[15−18] Generally, a Cu(I)−ligand complex and high monomer concentration are necessary to maximize polymer growth,[19−21] which highly relies on the reversible redox activation/deactivation of Cu(I)/Cu(II). Control over the Cu(I)/Cu(II) ratio is important to obtain fast a polymerization rate while prolonging the lifetime of propagation chains.[22,23]

The scope of ATRP has been expanded to external stimulus-induced polymerizations,[24,25] such as in electrochemically mediated ATRP (eATRP) for controlling polymerization by the electrically one-electron reduction of air-stable Cu(II).[26,27] We extended the eATRP technique to surface-initiated eATRP for controllable fabrication of surface-attached polymer brushes.[28] External visible light-stimulated living radical polymerization has been proposed through the excited Ir(III) species to reduce an alkyl bromide initiator for alkyl radical formation to initiate polymerization,[29,30] click reaction,[31,32] light-mediated atom-transfer radical addition,[33] and photo-iniferter-mediated surface attached polymers formation.[34] The key to external stimulus-induced polymerization is continuous in situ generation of the activator catalyst. In this report, we propose a novel approach to achieve surface-initiated ATRP with multiple usage of monomer solutions, wherein the polymerization activators, Cu(I)−ligand, can be continuously generated from a photochemical reduction process by the excited electrons under ultraviolet (UV) illumination that uses the TiO_2 nanoparticle as the photosensitive material.

Scheme 1. (a) Schematic Setup to Perform UV-ATRP and Structure of the Thiol Initiator and (b) Mechanism of UV Light-Induced Surface-Initiated Atom Transfer Radical Polymerization and Structure of the Thiol Initiator

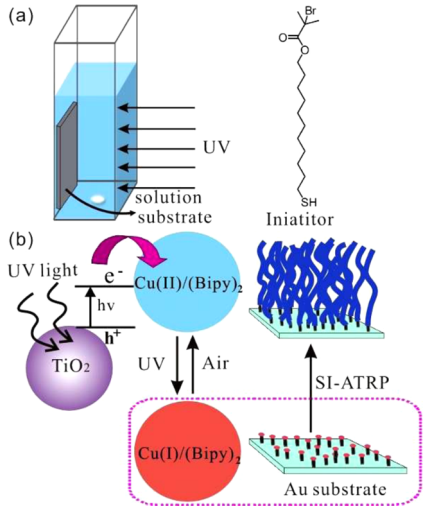

Scheme 2. Mechanism of UV Light-Induced ATRP

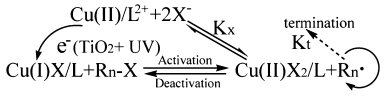

Scheme 1(b) displays the mechanism of UV light-induced ATRP. A commercially available TiO_2 nanoparticle, P25, was

Received: May 13, 2013
Accepted: June 11, 2013
Published: June 12, 2013

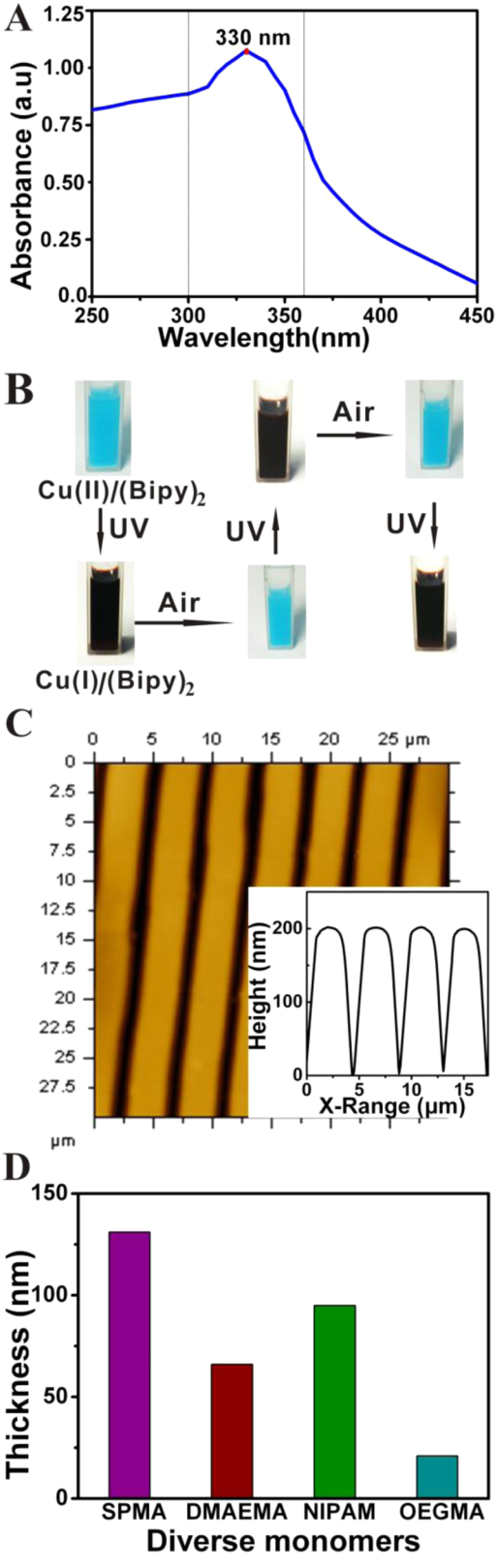

Figure 1. (A) UV−Vis spectra of annealed P25. (B) Digital photograph of the polymerization solution by alternating UV irradiation and exposure to air. (C) AFM image of 200 nm thick PSPMA brushes obtained after 2 h of polymerization (P25 concentration: 10 mg/mL; light intensity: 1.25 mW/cm^2). (D) Thickness of polymer brushes obtained from several monomers after 1 h UV-ATRP at room temperature (P25 concentration: 10 mg/mL; light intensity: 1.25 mW/cm^2).

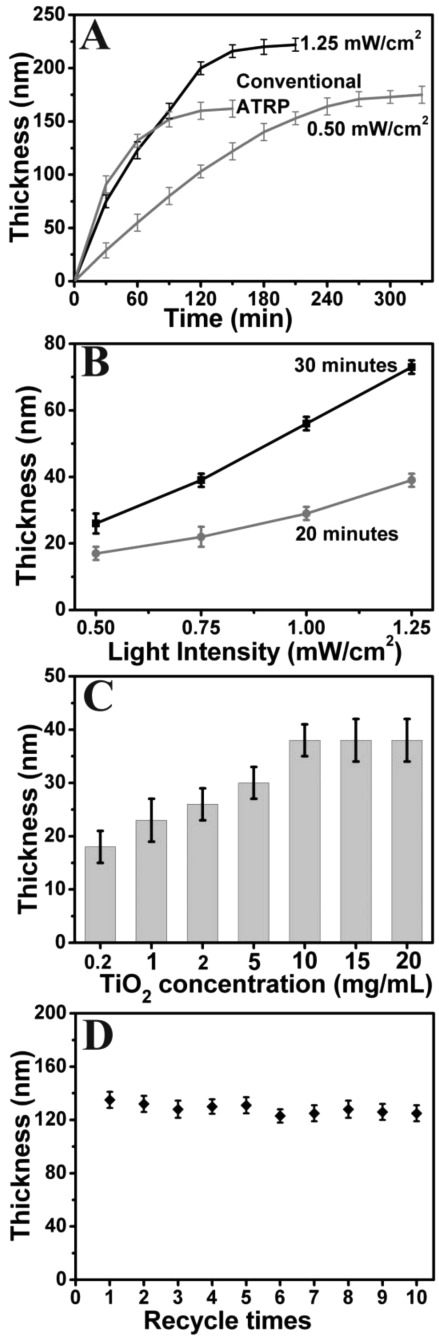

Figure 2. (A) First-order kinetics with respect to SPMA monomer growth on Br−C15−thiol-patterned gold surfaces at different light intensities (P25 concentration: 10 mg/mL) and under conventional ATRP (3 g of SPMA + 5 mL of 2:1 (v/v) H_2O/MeOH + 35 mg of bipy + 12 mg of CuBr). (B) Effect of UV light intensity on PSPMA brush thickness at different exposure times of 20 and 30 min (P25 concentration: 10 mg/mL, wavelength: 330 nm). (C) Thickness of PSPMA brushes versus P25 concentration at 1.25 mW/cm^2 illumination for 20 min. (D) Repeated use of SPMA solution (UV-ATRP for 1 h, P25 concentration: 10 mg/mL; light intensity: 1.25 mW/cm^2 at 330 nm wavelength).

used as a low-cost UV-absorbing material. During UV illumination, this material easily absorbs photons and promotes electrons from the valence bands to the conduction bands, and then the electrons will be promoted. The excited electrons can spontaneously reduce Cu(II)−ligand to Cu(I)−ligand, which

dx.doi.org/10.1021/mz400237w | ACS Macro Lett. 2013, 2, 592−596

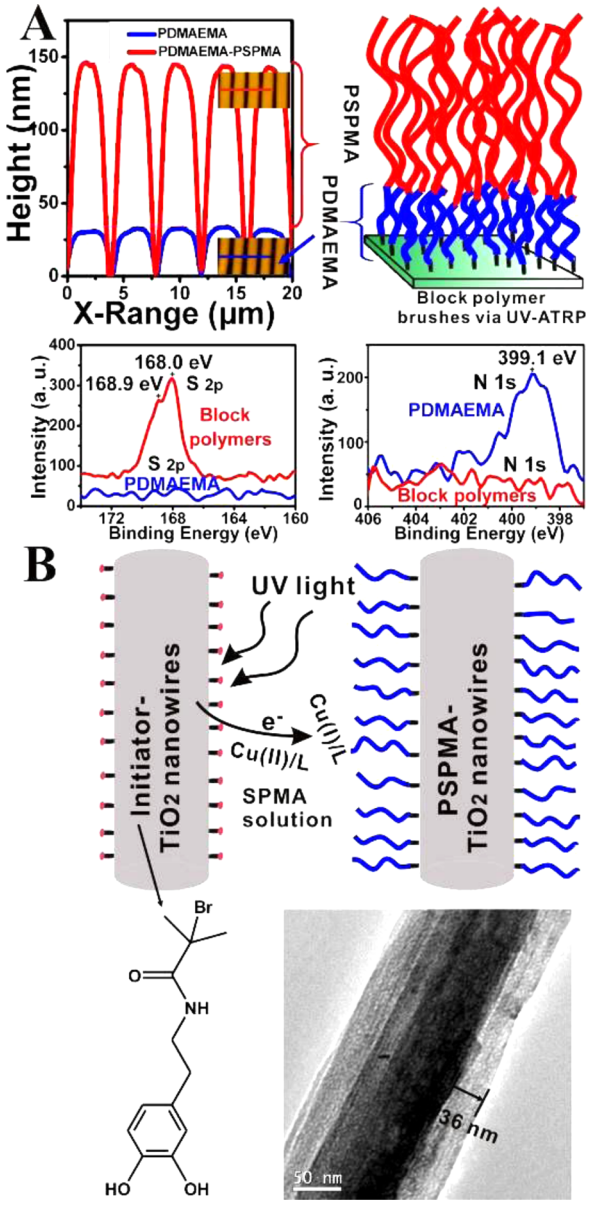

Figure 3. (A) Left image is an AFM image showing the line traces of the PDMAEMA and PSPMA-PDMAEMA brushes. The right image is a schematic illustration of PSPMA-PDMAEMA brushes generated by UV-ATRP. High-resolution XPS spectra of S 2p and N 1s of PDMAEMA and PSPMA-PDMAEMA brushes underneath (P25 concentration: 10 mg/mL; light intensity: 1.25 mW/cm^2). (B) The upper image shows a schematic illustration of the mechanism of self-catalytic UV-ATRP on TiO_2 nanowires, and the bottom image shows a TEM image of PSPMA brush-modified TiO_2 nanowires and structure of the initiator (initiator−TiO_2 nanowire concentration: 10 mg/mL; light intensity: 1.25 mW/cm^2).

reacts with alkyl halide (RX) to produce radicals (R$^\bullet$) for initiating polymerization; Cu(I) turns to the high valence state to complete a cycle (Scheme 2). Holes can be consumed to oxidize methanol in the medium.[35] Generally, Cu(I)/bipy prefers an octahedral ligand sphere, thus $Cu(bipy)_3^+$ and $Cu(bipy)_2X$ are its main form. Cu(II) species prefer a tetrahedral ligand sphere, $Cu(bipy)_2^{2+}$.[36] The excess Cu(I) catalyst used in conventional aqueous ATRP often results in high alkyl radical concentration and poor controllability of polymerization. As well, the halidophilicity of Cu(II)/L^{2+} lowers the concentration of the deactivator X−Cu(II)L^+, allowing less control of the polymerization. Ideal aqueous ATRP should account for all of these aspects.[27] Activators generated by electron-transfer ATRP[37,38] exert relatively better control over the targeted degree of polymerization but require very precise control of the ratio of the Cu(II)/reducing agent. Optimal polymerization necessitates a constant and relatively high Cu(II)/Cu(I) ratio. In UV-ATRP, the concentration of P25 and light intensity can be easily modulated, thereby facilitating the adjustment of ATRP and more controllable polymer grafting. Wasted monomer solutions can be reused as an easy and cost-effective method of growing different polymer brushes with desired architectures. UV-ATRP was performed in a square quartz cuvette with Cu(II)/L, P25, and monomer solution (Scheme 1(a)). After removal of oxygen via Ar flow, an initiator-modified Au substrate was placed vertically in the solution and illuminated by UV-light-reduced Cu(II)/L and initiated polymerization. At various time points, the substrates were removed from the solution and washed with copious amounts of ultrapure water and ethanol.

P25 is an anatase nanoparticular material with a size range of 10−40 nm (XRD and TEM in Figure S2 in Supporting Information). Figure 1A shows the peak absorbance of P25 at 330 nm in water/methanol, as determined from its UV−vis spectrum. Figure 1B shows a diagram of a digital photograph of polymerization solution of UV-ATRP based on alternating UV irradiation and air bubbles during the polymerization of a 3-sulfopropyl methacrylate potassium salt (SPMA) monomer in a conventional $Cu(bipy)_2^{2+}$ solution. The polymerization solution turned from light blue to dark brown in a certain time point during UV light exposure (330 nm, intensity: 1.25 mW/cm^2) because of the simultaneous reduction reaction of $Cu(bipy)_2^{2+}$ to $Cu(bipy)_2X$ upon ATRP initiation. The polymerization solution turned back to light blue upon exposure to air, indicating that the $Cu(bipy)_2X$ had been oxidized to its initial state. This reversible process can be repeated many times. Figure 1C shows a typical atomic force microscope (AFM) image of the patterned PSPMA brushes on a Au surface prepared from a prepatterned initiator using microcontact printing.[15] UV-ATRP yielded polymer brushes of about 200 nm thickness after 2 h of polymerization, which indicated that UV light induced surface grafting was an efficient approach to realize a higher thickness.[39] Many other monomers (Figure S1, Supporting Information) can also be polymerized by UV-ATRP, such as 2-(dimethylamino)ethyl methacrylate (DMAEMA), *N*-isopropylacrylamide (NIPAM), and oligo-(ethylene glycol) methacrylate (OEGMA) (Figure 1D).

$$R_p = k_p K_{eq}\left(\frac{[R_nX][Cu(I)/L][M]}{[X - Cu(II)/L]}\right) \quad (1)$$

The polymerization rate of ATRP was determined by the concentration of Cu(I)/Cu(II) species according to eq 1. Theoretically, the amount of in situ generated Cu(I) ions can be controlled by adjusting the light intensity and the Cu(I)/Cu(II) ratio, which has a direct relationship with the number of activated chain ends and the capability for deactivation (Scheme 2). Polymer growth kinetics at different light densities was investigated, and the results are shown in Figure 2A and Figure 2B. Extended UV irradiation gradually increased polymer thickness, and the polymer growth leveled off after 2 h at 1.25 mW/cm^2. Polymer thickness reached over 200 nm. Polymer growth occurred slightly slower but in a more linear

dx.doi.org/10.1021/mz400237w | ACS Macro Lett. 2013, 2, 592−596

manner than the conventional ATRP catalyzed directly by Cu(I)/L, which exhibits polymer growth leveling off at around 1 h and a yield of only 150 nm brushes (Figure 2A). This result can be attributed to the small amount of $Cu(bipy)_2X$ generated at the first stage of UV illumination and the high $Cu(bipy)_2^{2+}$ concentration in the solution, which is beneficial for retaining a small number of propagating chains and its deactivation by high-concentration $Cu(bipy)_2^{2+}$ species theoretically. Termination probability was significantly reduced because of the low concentration of free radicals; thus polymerization was more controlled and could be prolonged.[20,36] It is likely that the $Cu(bipy)_3^+$ concentration continuously increased to gain more initiation points. Therefore, at low irradiation intensity, the polymerization rate is slower but more controlled. This supposition was further confirmed by carrying out polymerization at low light intensity (i.e., 0.5 mW/cm^2), during which polymer brushes grew slower at 1.25 mW/cm^2 (Figure 2A). However, the polymerization time for linear brush growth at 0.5 mW/cm^2 irradiation (4 h) was much longer than that at 1.25 mW/cm^2 (2 h).

Light intensity affects the polymerization rate by changing the generation rate of the $Cu(bipy)_2X$. Higher illumination intensity containing more photons increases the generation amount of electrons, which can accelerate the $Cu(bipy)_2X$ generation rate. Figure 2B shows that the thickness of polymer brushes can be regulated by varying the irradiation intensity at 330 nm at different times. The polymer brushes grew more rapidly at higher light intensity, thereby providing a new externally controlled protocol for adjusting the polymer growth. Another factor that can affect the grafting kinetics is the P25 concentration, which determines the amount of $Cu(bipy)_2X$ produced at a certain light intensity. Figure 2C shows the brush thickness at 1 mW/cm^2 illumination for 20 min under different P25 contents. At very low P25 concentration, such as 0.2 mg/mL, the polymer growth rate is slow because of the small amount of $Cu(bipy)_2X$ produced, as indicated by the slight brownish red color of the polymerization solution. With increasing P25 concentration, brush thickness gradually increased until a maximum value was achieved at 10−15 mg/mL of P25. Further increases in P25 concentration to 20 mg/mL did not benefit the polymer growth, probably because the maximal photoreduction efficiency had been achieved. Low light intensity and lower P25 concentration also helped maintain a high Cu(II)/Cu(I) ratio to prolong the polymerization time for linear brush growth (Figure S4A in Supporting Information). The monomer solution can be repeatedly used many times. Figure 2D shows the PSPMA brushes grown from the same stock solutions. These brushes had almost the same thickness after 10 repeat polymerizations. In each cycle of surface grafting polymerization, only a very small portion of the monomer was consumed, and the monomer concentration exhibited almost no change. Thus, the solutions can be reused many times without affecting the polymer growth kinetics.

A swelling experiment was performed to compare the PSPMA brushes prepared by UV-ATRP and those obtained from conventional surface-initiated ATRP. The UV-ATRP brushes had a larger swelling ratio ($h_{swollen}/h_{dry}$ = 3.04) than those obtained by the conventional method ($h_{swollen}/h_{dry}$ = 2.18; Figure S3D and Figure S3E in Supporting Information). A larger swelling ratio indicates a higher degree of polymerization at the same dry thickness[40] and a smaller grafting density. The molecular weight (Mr) and polydispersity index (PDI) of the surface attached polymers were extremely difficult to measure because of the small amount of grafted materials.[41]

The living nature of the polymerization was confirmed by its ability to form copolymer brushes. PDMAEMA brushes at 30 nm were grafted via a 30 min polymerization procedure, after which PSPMA brushes were grafted onto their ends. The as-prepared samples were sufficiently washed with water and ethanol. Figure 3A shows a schematic of the block-polymer brushes. As illustrated from the AFM cross-section line trace, the second polymerization yielded block polymer brushes 150 nm thick. A high-resolution X-ray photoelectron spectroscopy (XPS) spectrum confirmed the N 1s signal at 399.1 eV after PDMAEMA grafting. This signal disappeared after the second grafting. The appearance of duplet S_{2p} signals at 168.0 eV ($S2p_{3/2}$) and 168.9 eV ($S2p_{1/2}$) and the disappearance of the N_{1s} peak verified the presence of block polymer brushes. Using multiple contact printed initiator[15] and UV-ATRP, we can prepare multicomponent surfaces on which different polymer brushes can sit side by side on a single surface (Figure S6, Supporting Information).

Interestingly, self-catalytic UV-ATRP can occur in nanostructured TiO_2, which acts as both the sensitizer and the substrate. The catecholic initiator (Figure 3B) self-assembled on TiO_2 nanowires and was added to the Cu(II)/L and SPMA monomer solution under UV light to generate catalysis and enable brush growth. Figure 3B shows the mechanism of self-catalytic UV-ATRP on catecholic initiator-modified TiO_2 nanowires (i.e., nanowires and nanotubes; Supporting Information for experiment details and Figure S7 and Figure S8). Figure 3B shows that after 1 h polymerization a PSPMA brush film of 36 nm was grafted onto the TiO_2 nanowires.

In summary, light-modulated surface-initiated ATRP was demonstrated. Polymer growth can be manipulated by either varying the content of photoactive materials or regulating the irradiation intensity of light, which changes the concentration of the catalytic Cu(I)−ligand. The monomer solution can be reused, and secondary polymerization can be performed to obtain block polymer brushes, indicating the living nature of the process. Thus, a method for forming well-defined polymer brushes for surface functionalization is introduced.

■ ASSOCIATED CONTENT

Supporting Information

Experimental details and additional characterization data. This material is available free of charge via the Internet at http://pubs.acs.org.

■ AUTHOR INFORMATION

Corresponding Author

*E-mail: zhouf@licp.cas.cn.

Notes

The authors declare no competing financial interest.

■ ACKNOWLEDGMENTS

Financial support from NSFC (21125316) and the Key Research Program of CAS (KJZD-EW-M01).

■ REFERENCES

(1) Barbey, R.; Lavanant, L.; Paripovic, D.; Schüwer, N.; Sugnaux, C.; Tugulu, S.; Klok, H.-A. *Chem. Rev.* **2009**, *109*, 5437.

(2) (a) Ye, Q.; Zhou, F.; Liu, W. *Chem. Soc. Rev.* **2011**, *40*, 4244. (b) Cheesman, B. T.; Willott, J. D.; Webber, G. B.; Edmondson, S.; Wanless, E. J. *ACS Macro Lett.* **2012**, *1*, 1161. (c) Nese, A.; Li, Y.;

Averick, S.; Kwak, Y.; Konkolewicz, D.; Sheiko, S. S.; Matyjaszewski, K. *ACS Macro Lett.* **2012**, *1*, 227.
(3) Chen, T.; Ferris, R.; Zhang, J.; Ducker, R.; Zauscher, S. *Prog. Polym. Sci.* **2010**, *35*, 94.
(4) Stuart, M. A. C.; Huck, W. T. S.; Genzer, J.; Müller, M.; Ober, C.; Stamm, M.; Sukhorukov, G. B.; Szleifer, I.; Tsukruk, V. V.; Urban, M.; Winnik, F.; Zauscher, S.; Luzinov, I.; Minko, S. *Nat. Mater.* **2010**, *9*, 101.
(5) Laloyaux, X.; Fautré, E.; Blin, T.; Purohit, V.; Leprince, J.; Jouenne, T.; Jonas, A. M.; Glinel, K. *Adv. Mater.* **2010**, *22*, 5024.
(6) Ma, H.; Hyun, J.; Stiller, P.; Chilkoti, A. *Adv. Mater.* **2004**, *16*, 338.
(7) Dalsin, J. L.; Hu, B.-H.; Lee, B. P.; Messersmith, P. B. *J. Am. Chem. Soc.* **2003**, *125*, 4253.
(8) Dunlop, I. E.; Briscoe, W. H.; Titmuss, S.; Jacobs, R. M. J.; Osborne, V. L.; Edmondson, S.; Huck, W. T. S.; Klein, J. *J. Phys. Chem. B* **2009**, *113*, 3947.
(9) Edmondson, S.; Osborne, V. L.; Huck, W. T. S. *Chem. Soc. Rev.* **2004**, *33*, 14.
(10) (a) Hawker, C. J.; Bosman, A. W.; Harth, E. *Chem. Rev.* **2001**, *101*, 3661. (b) Iha, R. K.; Wooley, K. L.; Nyström, A. M.; Burke, D. J.; Kade, M. J.; Hawker, C. J. *Chem. Rev.* **2009**, *109*, 5620. (c) Hawker, C. J.; Wooley, K. L. *Science* **2005**, *309*, 1200.
(11) Boyer, C.; Bulmus, V.; Davis, T. P.; Ladmiral, V.; Liu, J.; Perrier, S. *Chem. Rev.* **2009**, *109*, 5402.
(12) (a) Osborne, V. L.; Jones, D. M.; Huck, W. T. S. *Chem. Commun.* **2002**, 1838. (b) Xiao, D.; Wirth, M. J. *Macromolecules* **2002**, *35*, 2919.
(13) Ma, H.; Wells, M.; Beebe, T. P.; Chilkoti, A. *Adv. Funct. Mater.* **2006**, *16*, 640.
(14) (a) Zhang, Y.; Wang, Y.; Peng, C.-h.; Zhong, M.; Zhu, W.; Konkolewicz, D.; Matyjaszewski, K. *Macromolecules* **2012**, *45*, 78. (b) Wang, J.-S.; Matyjaszewski, K. *J. Am. Chem. Soc.* **1995**, *117*, 5614.
(15) Zhou, F.; Zheng, Z.; Yu, B.; Liu, W.; Huck, W. T. S. *J. Am. Chem. Soc.* **2006**, *128*, 16253.
(16) Bao, Z.; Bruening, M. L.; Baker, G. L. *J. Am. Chem. Soc.* **2006**, *128*, 9056.
(17) Yameen, B.; Kaltbeitzel, A.; Langner, A.; Duran, H.; Müller, F.; Gösele, U.; Azzaroni, O.; Knoll, W. *J. Am. Chem. Soc.* **2008**, *130*, 13140.
(18) Chen, T.; Amin, I.; Jordan, R. *Chem. Soc. Rev.* **2012**, *41*, 3280.
(19) Wang, X.-S.; Lascelles, S. F.; Jackson, R. A.; Armes, S. P. *Chem. Commun.* **1999**, 1817.
(20) Matyjaszewski, K. *Macromolecules* **2012**, *45*, 4015−4039.
(21) Sui, X.; Zapotoczny, S.; Benetti, E. M.; Memesa, M.; Hempenius, M. A.; Vancso, G. J. *Polym. Chem.* **2011**, *2*, 879.
(22) Tang, W.; Tsarevsky, N. V.; Matyjaszewski, K. *J. Am. Chem. Soc.* **2006**, *128*, 1598.
(23) Tang, W.; Kwak, Y.; Braunecker, W.; Tsarevsky, N. V.; Coote, M. L.; Matyjaszewski, K. *J. Am. Chem. Soc.* **2008**, *130*, 10702.
(24) (a) Tasdelen, M. A.; Ciftci, M.; Yagci, Y. *Macromol. Chem. Phys.* **2012**, *213*, 1391. (b) Tasdelen, M. A.; Uygun, M.; Yagci, Y. *Macromol. Chem. Phys.* **2011**, *212*, 2036. (c) Tanabe, M.; Guido, W. M. V.; Chan, W. Y.; Cyr, P. W.; Vanderark, L.; Rider, D. A.; Manners, I. *Nat. Mater.* **2006**, *5*, 467. (d) Yagci, Y.; Jockusch, S.; Turro, N. J. *Macromolecules* **2010**, *43*, 6245.
(25) (a) Konkolewicz, D.; Schröder, K.; Buback, J.; Bernhard, S.; Matyjaszewski, K. *ACS Macro Lett.* **2012**, *1*, 1219. (b) Wong, E. H. H.; Guntari, S. N.; Blencowe, A.; van Koeverden, M. P.; Caruso, F.; Qiao, G. G. *ACS Macro Lett.* **2012**, *1*, 1020. (c) Alfredo, N. V.; Jalapa, N. E.; Morales, S. L.; Ryabov, A. D.; Lagadec, R. L.; Alexandrova, L. *Macromolecules* **2012**, *45*, 8135.
(26) Magenau, A. J.; Strandwitz, N. C.; Gennaro, A.; Matyjaszewski, K. *Science* **2011**, *332*, 81.
(27) Bortolamei, N.; Isse, A. A.; Magenau, A. J.; Gennaro, A.; Matyjaszewski, K. *Angew. Chem., Int. Ed.* **2011**, *50*, 11391.
(28) Li, B.; Yu, B.; Huck, W. T. S.; Zhou, F.; Liu, W. *Angew. Chem., Int. Ed.* **2012**, *51*, 5092.
(29) (a) Fors, B. P.; Hawker, C. J. *Angew. Chem., Int. Ed.* **2012**, *51*, 8850. (b) Fors, B. P.; Hawker, C. J. *Angew. Chem.* **2012**, *124*, 8980.
(30) Leibfarth, F. A.; Mattson, K. M.; Fors, B. P.; Collins, H. A.; Hawker, C. J. *Angew. Chem., Int. Ed.* **2013**, *52*, 199.
(31) Tasdelen, M. A.; Yilmaz, G.; Iskin, B.; Yagci, Y. *Macromolecules* **2012**, *45*, 56.
(32) Harmand, L.; Cadet, S.; Kauffmann, B.; Scarpantonio, L.; Batat, P.; Jonusauskas, G.; McClenaghan, N. D.; Lastécouères, D.; Vincent, J. M. *Angew. Chem., Int. Ed.* **2012**, *51*, 7137.
(33) Wallentin, C. J.; Nguyen, J. D.; Finkbeiner, P.; Stephenson, C. R. J. *J. Am. Chem. Soc.* **2012**, *134*, 8875.
(34) (a) Harris, B. P.; Metters, A. T. *Macromolecules* **2006**, *39*, 2764. (b) Liu, Q.; Singh, A.; Liu, L. *Biomacromolecules* **2013**, *14*, 226. (c) Krause, J. E.; Brault, N. D.; Li, Y.; Xue, H.; Zhou, Y.; Jiang, S. *Macromolecules* **2011**, *44*, 9213.
(35) Takada, K.; Miyazaki, T.; Tanaka, N.; Tatsuma, T. *Chem. Commun.* **2006**, 2024.
(36) Matyjaszewski, K.; Xia, J. *Chem. Rev.* **2001**, *101*, 2921.
(37) Oh, J. K.; Min, K.; Matyjaszewski, K. *Macromolecules* **2006**, *39*, 3161.
(38) Simakova, A.; Averick, S. E.; Konkolewicz, D.; Matyjaszewski, K. *Macromolecules* **2012**, *45*, 6371.
(39) (a) Dyer, D. J.; Feng, J.; Schmidt, R.; Wong, V. N.; Zhao, T.; Yagci, Y. *Macromolecules* **2004**, *37*, 7072. (b) Gam-Derouich, S.; Lamouri, A.; Redeuilh, C.; Decorse, P.; Maurel, F.; Carbonnier, B.; Beyazıt, S.; Yilmaz, G.; Yagci, Y.; Chehimi, M. M. *Langmuir* **2012**, *28*, 8035.
(40) Tran, Y.; Auroy, P.; Lee, L.-T. *Macromolecules* **1999**, *32*, 8952.
(41) Turgman-Cohen, S.; Genzer, J. *J. Am. Chem. Soc.* **2011**, *133*, 17567.